Journal of Japan Association for Earthquake Engineering, Vol.8, No.4, 2008

DESIGN EARTHQUAKE GROUND MOTIONS FROM PROBABILISTIC RESPONSE SPECTRA: CASE STUDY OF NEPAL

Hari PARAJULI[1], Junji KIYONO[2] , Yusuke ONO[3] and Takahiro TSUTSUMIUCHI[4]

[1] Ph. D. student, Dept. of Urban Management, Kyoto University, Kyoto, Japan,
parajuli@quake2.kuciv.kyoto-u.ac.jp
[2] Member of JAEE, Associate Professor, Dept. of Urban Management, Kyoto University, Kyoto, Japan,
kiyono@quake.kuciv.kyoto-u.ac.jp
[3] Member of JAEE, Assistant Professor, Dept. of Urban Management, Kyoto University, Kyoto, Japan,
ysk@quake2.kuciv.kyoto-u.ac.jp
[4] Master student, Dept. of Urban Management, Kyoto University, Kyoto, Japan,
tsutsumiuchi@quake2.kuciv.kyoto-u.ac.jp

ABSTRACT: Probabilistic hazard estimate through out Nepal considering historical earthquakes, intra plate slip and faults are done. As a typical case probabilistic spectra are plotted for Pokhara city. For the city, design earthquakes for three probabilities of exceedences are simulated which can be useful to design new structures and retrofit of existing structures.

Key Words: Faults, historical earthquakes, kernel, response spectra, design earthquakes

INTRODUCTION

Nepal takes approximately half length of greater Himalaya, which is part of the trans-alpine belt, regarded as one the main earthquake prone zones of the world. Because of tectonic movement, many earthquakes have occurred in this region in its history. Records noted on some Nepalese religious tracts indicate that a big earthquake hit Kathmandu in June 1255 AD. The quake killed approximately one-third of its population at that time. Since then severe earthquakes have been reported which occurred in 1405, 1408, 1681, 1810, 1833, 1866 and 1934 AD (BECA 1993, Ambraseys and Douglas 2004). Evidences of a big earthquake in central part of Nepal occurred in the period from 700 to 1100 AD have been published recently but exact occurred date has not conformed yet (Lave et al. 2005). Historical records show that at least as far back as the early 18th century, damaging earthquakes have occurred in the Himalayan region in every few decades. But since 1950, the damaging earthquakes have not been reported in the region and in some areas. From recent studies depending upon the various analyses and GIS (Geographical Information System) data, slip rate of Indian and Tibetan plates is 19 mm per year (Jouanne et al. 2004). But the calculated slip for whole Himalyan-arc from occurred earthquakes is only one third of the observed slip (Bilham and Ambrasseys 2005). It shows that either the earthquake records are missing or severe earthquakes may be overdue. Many earthquakes struck greater Himalayan region in past but the worst may be yet to come and it may occur in or near Nepal. According to the new analysis by Bilham and Ambrssseys 2005, one or more massive earthquakes measuring greater than M8 on Richter scale may be overdue in the Himalaya, threatening the millions of people that live in the region.

More than ten thousand people were killed in 1934 earthquake. Since then, Nepal's population has doubled and urban population has increased by a factor of more than ten since last great earthquake. In urban, most of the people live in poorly constructed houses without considering the seismic codes. In rural area almost all people live in low strength masonry houses constructed by mainly by stones and bricks which have been proved the major cause of live loss in earthquakes. Considering past human tolls from earthquakes, population increases that have occurred since then and the added low quality houses, the future scenario of deaths and damages could be worse than 2005 Pakistan earthquake. Previous seismic hazard estimate (BECA 1993) is based on uniform distribution of assumed earthquakes data over big area without well explained details. That study does not consider the earthquakes greater than magnitude 8 whereas their catalogue also has earthquakes greater than that magnitude. Thus, revising all earthquake data, selecting suitable attenuation law, peak ground and spectral accelerations are estimated and contours are plotted for the region. For a site, contribution to particular value of acceleration by various magnitudes and distances are disaggregated. For all bins significant durations are calculated. Weighted average duration and envelope function are obtained by multiplying disaggregated hazard by significant duration. Design earthquake is estimated for calculated weighted average duration fitting with obtained probabilistic spectra. The whole procedure is shown in flow chart (Fig. 1).

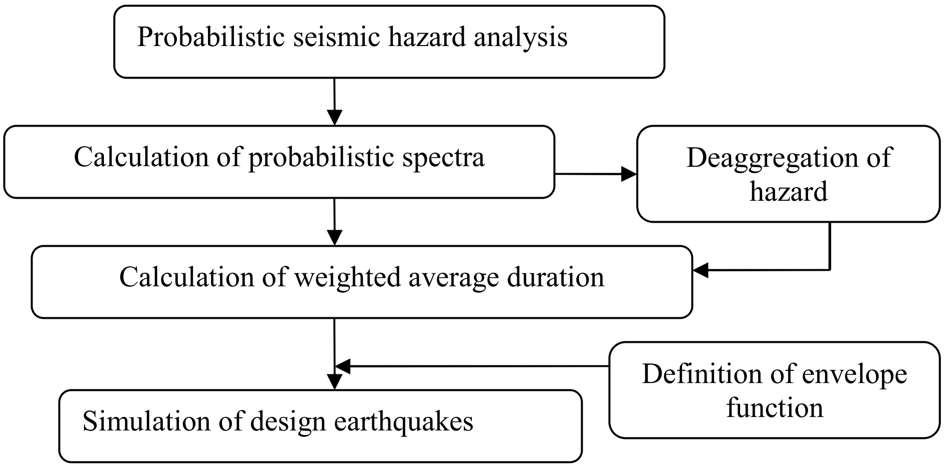

Fig. 1 Flow chart for simulation process

MAGNITUDE FREQUENCY RELATIONSHIP

Usual practice to develop earthquake frequency relationship is to collect earthquakes, assign to nearest fault and make the relationship. The site consists of 92 faults (BECA 1993). Only few earthquakes are available, most of the faults find very few data and even some of them are empty (Fig. 2). Available earthquakes are arranged in various magnitudes and years (Table 1). All the faults and historical earthquakes greater than magnitude M3 around Nepal are plotted in Fig.2. They are scattered and concentrated out side the faults. Being faults are historical evidences; they can not be neglected even though earthquakes have not occurred in time span of data.

Instead of considering individual faults, area sources have been modeled and earthquake density at particular area cell is calculated considering both historical earthquakes and faults which lay in the cell by kernel method which is explained later. Earthquake catalogue was formed merging the data from U.S. Geological Survey, National earthquake Information Centre (NEIC), BECA 1993, Ambraseys and Douglas 2004 and Lave et al. 2005. Though historical earthquakes occurred in the region have been documented since 1100AD, earthquakes data have gone missing (Bilham and Ambrasseys 2005 and Jouanne et al. 2004) and available data are not sufficient to justify the current slip rate 19mm/year (Jouanne et al. 2004). Magnitude frequency relationship (eq. 2) has been developed (Parajuli et al. 2007) by calculating slope of the relationship from existing earthquakes and considering 50% intra-plate slip which clearly satisfies (Fig. 3) the rate of smaller and great earthquakes which is explained in the following paragraphs.

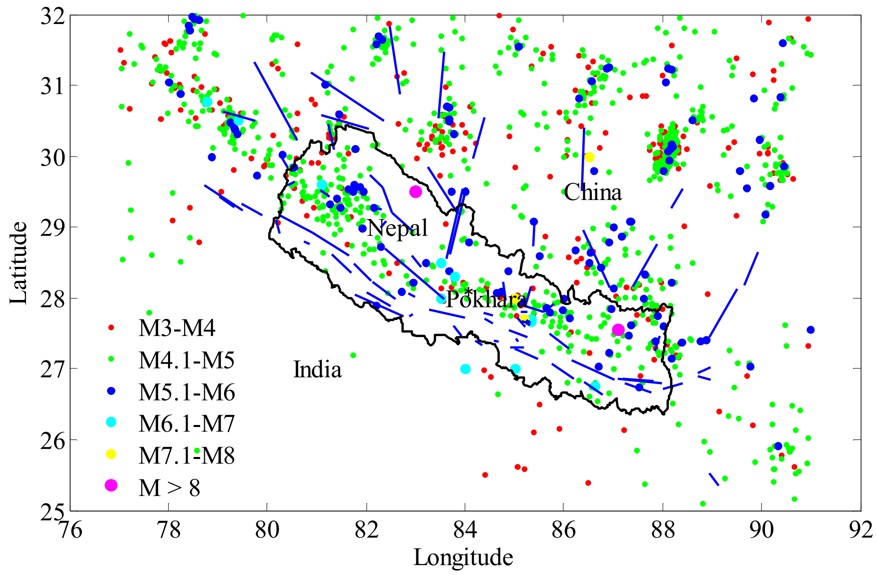

Fig. 2 Historical earthquakes (points) and faults (line)

Table 1 Arrangement of earthquake events

Year		Magnitude					Total
Start	End	4.0-4.9	5.0-5.9	6.0-6.9	7.0-7.9	8.0-8.9	
1100	1931	1	2	5	5	2	**15**
1932	1936	1	2	1	1	1	**6**
1937	1941		2				**2**
1942	1946		1				**1**
1947	1951		1				**1**
1952	1956		4	2			**6**
1957	1961		2				**2**
1962	1966	7	5	1			**13**
1967	1971	11	3	1			**15**
1972	1976	13	3				**16**
1977	1981	12					**12**
1982	1986	14					**14**
1987	1991	29	2	1			**32**
1992	1996	19	1	1			**21**
1997	2001	23	2				**25**
2002	2006	16					**16**
Total		**146**	**30**	**12**	**6**	**3**	**197**

Since the earthquake data have been reported in different magnitudes and intensity scales, all data were converted to moment magnitude (Hank and Kanamori 1979) using various relationships (McGuire 2004) and scaling relationship for Himalayan region (Ambraseys and Douglas 2004). The total 197earthquake events with magnitude greater than M4 are grouped as shown in table 1. The data are not uniformly distributed temporally. Analysis for temporal completeness was performed (Stepp 1972), with events grouped into small intervals of time. If k_1, k_2, k_3, ..k_n, are the number of quakes per unit time interval, then an unbiased estimate of the mean rate of earthquakes per unit time interval of the sample exceeding each magnitude is given by eq. 1. The rates of earthquakes exceeding each magnitude using eq. 1 are calculated (Table 2) and plotted in semi log scale (Fig. 3). The magnitude frequency relationship is represented by eq. 2.

$$rate_M = \frac{1}{n}\sum_{i=1}^{n} k_i \tag{1}$$

$$Log(N/Y) = 3.47 - 0.76M \tag{2}$$

Table 2 Mean rate of historical earthquakes

Magnitude exceeding	Year		Duration (years)	Average rate
	Start	End		
M4	1962	2006	32	3.97
M5	1932	2006	75	0.37
M6	1657	2006	350	0.069
M7	1255	2006	752	0.013
M8	1100	2006	602	0.003

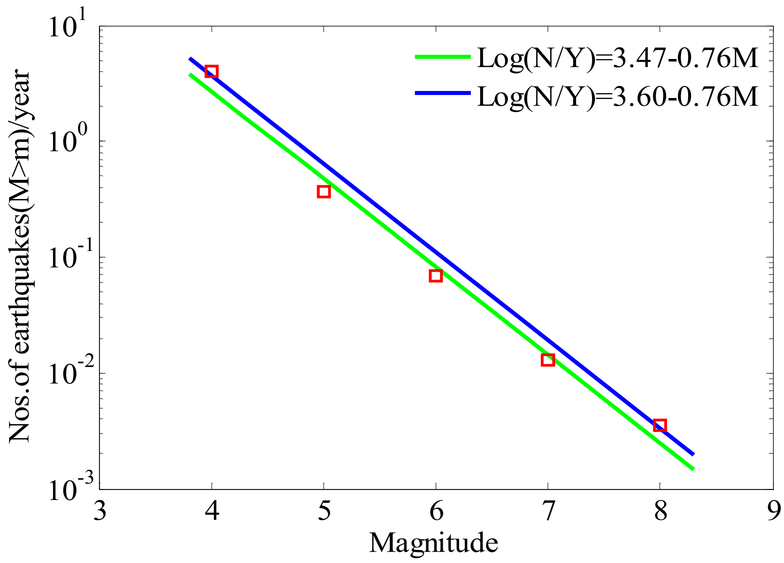

Fig. 3 Magnitude frequency relationship

The slope of magnitude frequency relationship (eq. 2) is less than 1 and shows high rate of occurrences of larger magnitude earthquakes. Though historical earthquakes in Nepal have been documented since 1100 AD, various researchers (Bilham et al. 2007, Feldl and Bilham 2006, Bilham and Ambrasseys 2005, Jouanne et al. 2004) have pointed out that an intra-plate slip deficit exists in the Himalayan region. The slip velocity between India and southern Tibet as measured by GPS measurement is 16-18 mm/year (Bilham et al. 1997) and the slip velocity of central and eastern Nepal is 19mm/year (Jouanne et al. 2004). The slip rate estimate (Bilham and Ambraseys 2005) based on 500 years of earthquake data accounts for only one third of the total seismic rate of the region, and the remaining slip deficit is equivalent to five earthquakes greater than M8.5.

The question therefore arises of whether this fit is sufficient to represent the seismicity of the region when a large slip deficit exists and the faults are sufficiently mature to sustain renewed rupture (Feldl and Bilham 2006) effectively, there is the possibility of a mega thrust event with 600km by 80km rupture area and more than 9m slip (Bilham and Ambraseys 2005). Slip rate ($\dot{s}$) can be obtained from moment rate ($\dot{M}_0$), shear modulus (μ) and fault area (A_f) using eqs. 3-6 (McGuire 2004).

$$\dot{s} = \frac{\dot{M}_0}{\mu A_f} \tag{3}$$

$$\dot{M}_0 = \frac{\nu_{M_{\min}} k\beta \exp\left[\beta\left(M_{\min} + 16.05/1.5\right)\right]}{\gamma - \beta}\left(M_{0_{\max}}^{1-\beta/\gamma} - M_{0_{\min}}^{1-\beta/\gamma}\right) \tag{4}$$

$$k = \left[1 - e^{-\beta\left(M_{\max} - M_{\min}\right)}\right]^{-1} \tag{5}$$

$$\nu_{M_{\min}} = 10^{\left(a - bM_{\min}\right)} \tag{6}$$

Where $\gamma = 3.454$ and $\beta = 2.303b$, and $M_{0_{\max}}$ and $M_{0_{\min}}$ are maximum and minimum moments corresponding to maximum and minimum magnitudes, calculated using eq. 7 (Hank and Kanamori 1979).

$$\log_{10} M_0 = 1.5M + 16.05 \tag{7}$$

Considering the lower threshold magnitude M5 and maximum magnitude M8.8 (Lave et al. 2005), fault area 600km by 80km, a and b (coefficients) values from eq. 2 and μ=3.3E11dyne/cm^2, the slip rate is 37% of total slip (1.9cm/year). Alternative explanations are possible for the apparent contradiction between observed data and slip velocity. Earthquake data may be missing, the magnitude value of the events may have been underestimated, the slip may be aseismic creep, or the current study period may not be long enough compared to the recurrence rate of great earthquakes. Efforts have been made to find missing data – for example, recently an earthquake in 1100 AD has been identified in eastern part of Nepal (Lave et al. 2005) and another one in Garhwal Himalaya (Kumar et al 2006).

Observing eq. 2, slip depends upon a, b values, area of fault and maximum magnitude. The main shortcoming of this magnitude frequency fit is that it is based on relatively few data. However, earthquake data are almost complete at magnitude M4, and the period of study since 1100 AD may not be sufficient for events greater than M8. As three earthquakes greater than M8 have been identified and the return period for these events is nearly 500 years (Feldl and Bilham 2006), the seismic hazard assessment should be based on the rates of these events. In that sense, considering the slope (b value) of the magnitude frequency relation and maximum magnitude are constant, and taking the same area as Bilham and Ambraseys 2005, an increased slip rate to 50% yields a (coefficient of magnitude frequency relation) value of 3.60, which closely matches the rate of occurrence of events greater than M8 and complete M4 (Fig. 3, blue line), so that the magnitude frequency relation can be represented by eq. 8.

$$Log\left(N/Y\right) = 3.60 - 0.76M \tag{8}$$

PROBABILISTIC SEISMIC HAZARD ASSESSMENT (PSHA)

Seismic hazard curve for each site can be obtained from summing up the mean rate of exceedences of all small source zones. N_s is the numbers of sources in the region, total mean rate exceedences (Kramer 1996) for the region is estimated by eq. 9.

$$\nu_{y^*} = \sum_{i=1}^{N_s}\sum_{j=1}^{N_r}\sum_{k=1}^{N_m} \nu_{i_{M\min}} \rho_i P\left[Y > y^* \mid m, r\right] P\left[M = m\right] P\left[R = r\right] \Delta m \Delta r \tag{9}$$

$$\rho_i = \frac{\lambda(m,x)_i}{\sum_{i=1}^{N_s} \lambda(m,x)_i} \tag{10}$$

where $P[Y > y^* \mid m, r]$ is conditional probability that ground motion parameter Y (acceleration) exceeds a particular value y^* using attenuation law for a given magnitude M and distance R, and $P[M = m]$ and $P[R = r]$ are probabilities of occurrence of particular magnitude and distance respectively. No specific attenuation law has been developed for Himalayan region. Atkinson and Boore 2003 compiled all earthquakes database added many recent earthquakes data from Japan through 2001, formed four times bigger database than others' for subduction zone events and developed new ground motion relation. It is the latest and includes all types of earthquakes and is selected in this study. Earthquake data has magnitude, distance and depths and can be directly used in attenuation law. For area sources, magnitude dependent parameter delta (Atkinson and Boore 2003) is taken as depth. Lengths of faults are taken from BECA 1993. Since, some of the faults do not hold any earthquake data, maximum magnitude calculated (Wells and Coppersmith 1994) for each faults were assigned as one equivalent earthquake while calculating density. Here, M and m are used as random variable and specific value for magnitude. Total area of 600kmx600km around each site is taken and divided into 120x120 cells. Distances between centre of cells and site are calculated. Only the cells within 300km radius are considered in the study. Magnitude is divided into 0.5M and distance into 5km intervals. N_m and N_r are the total numbers of magnitudes and distances bins. Earthquake densities (ρ_i) for each cell are considered using kernel estimation methods (Woo 1996). The mean activity rate $\lambda(m,x)$ satisfying $r \le h(m_j)$, at a cell x is taken as a kernel estimation sum considering the contribution of N events inversely weighted by its effective return period which can be obtained from eqs. 11-13.

$$\lambda(m,x)_i = \sum_{j=1}^{N} \frac{K(m_j, r_j)}{T(r_j)} \tag{11}$$

$$K(m,r)_j = \left[\frac{D}{2\pi h(m_j)}\right]\left\{\frac{h(m_j)}{r_j}\right\}^{2-D} \tag{12}$$

$$h(m_j) = H \exp(C m_j) \tag{13}$$

where, $K(m,x)$ is kernel function, $T(r)$ is return period of the event located at distance r, $h(m)$ is kernel band width scaling parameter shorter for smaller magnitude and vice-versa, which is regarded as fault length, D is fractal dimension, is taken as 1.7 , H and C are constants equals to 1.45 and 0.64.

PROBABILISTIC SPECTRA

Mean rate of exceedences of peak ground accelerations and spectral accelerations at various periods of vibration from all small sources are obtained from eq. 1 using Atkinson and Boore 2003 attenuation equation. Assuming earthquake occurrences obey Poisson's process, peak ground accelerations and spectral accelerations corresponding to 40%, 10% and 5% probabilities of exceedences in 50 years are determined. Distribution of peak ground accelerations over the country for the three different probability of exceedences which are equivalent to 98, 475 and 975 years return period respectively have been plotted in Figs.4-6. Figs. show that eastern and far western regions may experience bigger peak ground accelerations than in central regions. Two big (greater than M8) earthquake have occurred and lower magnitude historical earthquakes (Fig. 2) are also densely populated in these regions than in central region. Long faults are also in western and eastern side, however small faults are in central part. As a typical example, for Pokhara city, latitude 28.2N and longitude 83.98E, peak ground accelerations and spectral accelerations at various periods for soft soil condition are obtained (Fig. 7).

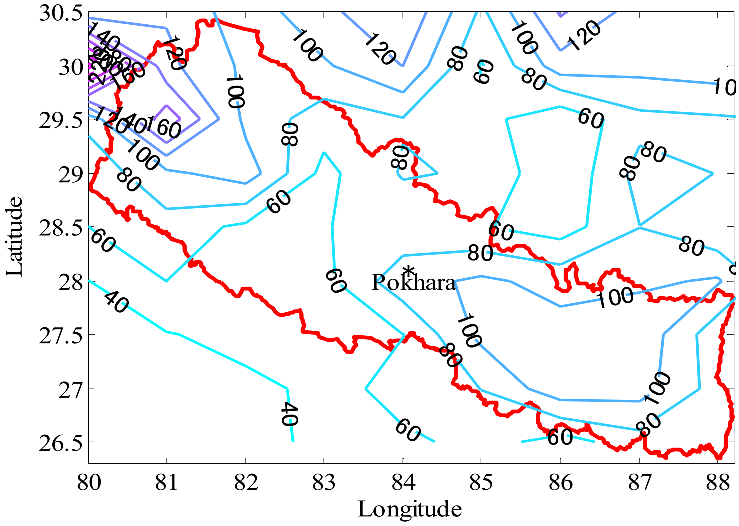

Fig. 4 Peak ground acceleration (gal) in 40% in 50 years (soft soil)

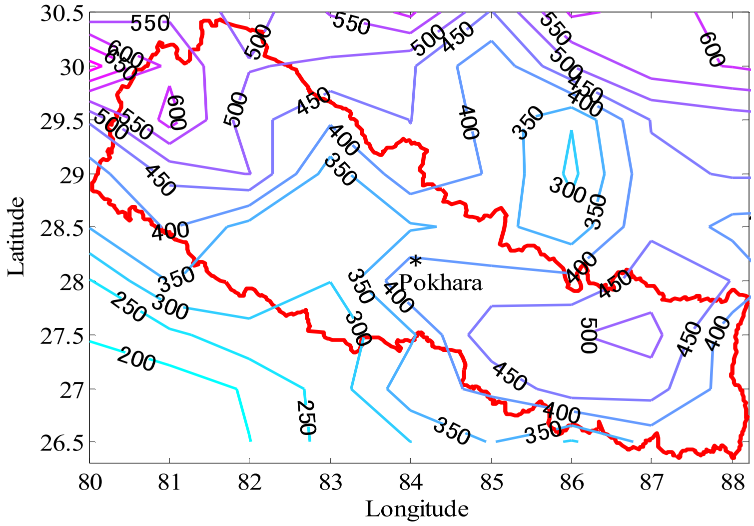

Fig.5 Peak ground acceleration (gal) in 10% in 50 years (soft soil)

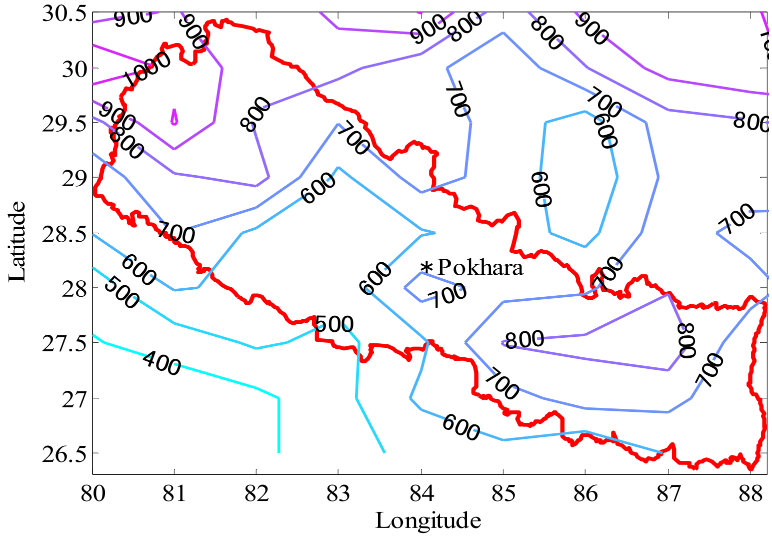

Fig. 6 Peak ground acceleration (gal) in 5% in 50 years (soft soil)

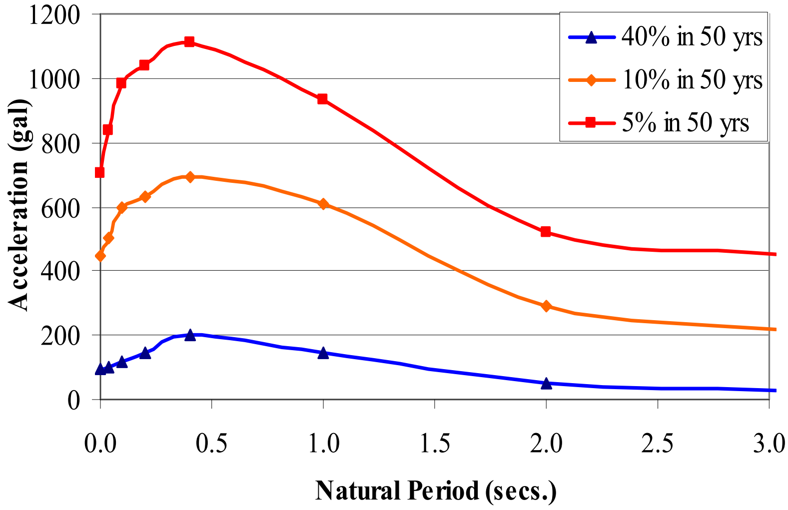

Fig. 7 Response spectra (5% damping) at Pokhara (soft soil)

DURATION AND ENVELOPE FUNCTION

Duration of earthquake is function of magnitude and epicentral distance, thus each earthquake has separate duration. A probabilistic spectrum consists of many earthquakes. Even within duration span acceleration amplitudes are not uniform. Thus total duration (T_D) is divided into three parts as shown in Fig.8. In the first part up to T_B acceleration will be ascending, between T_B to T_C, it is much effective and after T_C, it starts descending. T_B and T_C are calculated using equations following Osaki 1994 and

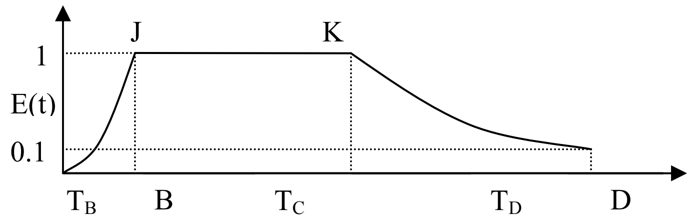

Fig. 8 Division of duration and envelope function

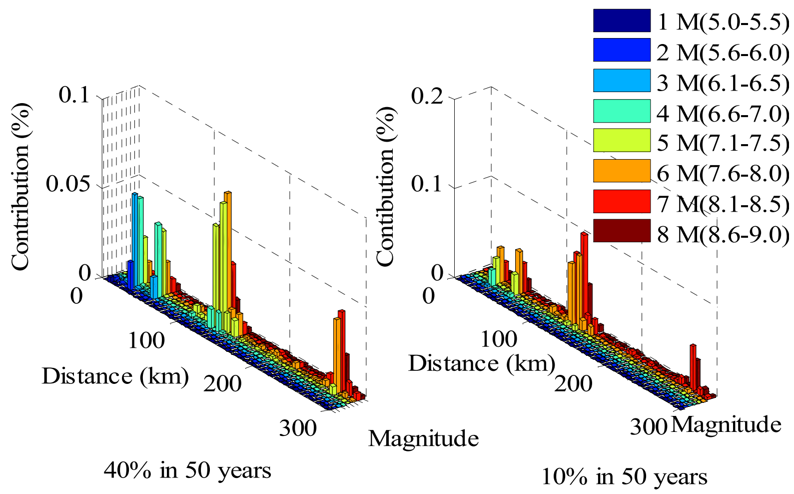

Fig. 9 Disaggregation PGA at Pokhara (soft soil)

T_D is calculated using equation following Kemption and Stewart 2006. It is significant duration which is defined as the time interval across which 5 to 95% of total energy is dissipated.

$$T_B = [0.12 - 0.04(M-7)]T_D \tag{14}$$

$$T_c = [0.50 - 0.04(M-7)]T_D \tag{15}$$

$$\ln T_D = \ln\left[\frac{\left(\frac{\exp(b_1 + b_2(M-6))}{10^{1.5M+16.05}}\right)^{-1/3}}{4.9.10^6\beta} + c_2 r + c_1 s\right] \tag{16}$$

where, b_1, b_2, c_1, c_2 are coefficients equal to 2.79, 0.82, 1.91, 0.15 respectively, β is shear wave velocity equal to 3.2km/sec. s is soil type and equal to 1 for soil, and zero for rock, M is magnitude of earthquake and r is epicentral distance. Now, envelope function E(t) is calculated using eqs. 17-19.

$$0 \le t \le T_B: \; E(t) = \left(t/T_B \right)^2 \tag{17}$$

$$T_B \le t \le T_c: \; E(t) = 1 \tag{18}$$

$$0 \le t \le T_B: \; E(t) = \exp\left(\frac{\ln 0.1}{T_D - T_C}(t - T_C) \right) \tag{19}$$

In order to find out appropriate duration, all accelerations are disaggregated in terms of magnitudes and distances (Fig. 9). Disaggregated cells have separate magnitudes, distances and weights. Separate significant durations for all cells using eqs. 14-16 were calculated, then, obtained durations are multiplied by corresponding cell's weight obtained from disaggregation and weighted durations are found summing up all bins' durations. We obtain duration for particular value of response acceleration corresponds to specific period. However, we need a single value applicable for all acceleration that fall in specified probability of exceedence in specified period of years. Thus, using similar procedure, durations for all accelerations are calculated. These calculated durations have combined effects of distance, magnitude and weight of deaggregation. For lower accelerations, contribution of lower magnitude earthquakes in hazard is significant but duration is short. For distant earthquakes duration is long but its contribution to hazard is low. For frequent earthquakes, smaller magnitude earthquake also contribute more but when probability decreases contribution of higher magnitude earthquake increases. In an average, the duration remains almost same for all earthquakes which fall in same return period. Thus, the weighted durations corresponding to same return period are in close margin. Then weighted average duration is calculated from all accelerations. For spectra shown in Fig. 7, durations are presented in Table 3.

Table 3 Weighted average duration for Pokhara

Durations	40% in 50 yrs	10% in 50 yrs	5% in 50 yrs
TD	30.0	45.0	51.0
TB	3.5	5.3	5.9
TC	15.0	23.0	26.0

DESIGN EARTHQUAKES

Design earthquakes are simulated for calculated durations (Table 3). Total duration is first divided into small interval dividing by number N as shown in eq. 20. Using incremental time, Fourier transform pair C_k and x_m are evaluated through eqs. 21-24.

$$\Delta t = \frac{T_D}{N} \tag{20}$$

$$C_k = \frac{1}{N}\sum_{m=0}^{N-1} x_m \exp\left(-i\left(2\pi km/N\right)\right), \text{ k=0, 1, 2, … , N-1} \tag{21}$$

$$x_m = \sum_{k=0}^{N-1} C_k \exp\left(i\left(2\pi km/N\right)\right), \text{ m=0, 1, 2, … , N-1} \quad 22)$$

$$C_k = F_k\left(\cos\phi_k + i\sin\phi_k\right) \tag{23}$$

$$R_d = \frac{S_{ds}}{S_{dt}} \tag{24}$$

where F_k is Fourier amplitude,ϕ is phase angle, R_d, is ratio of simulated (S_{ds}) to target spectra (S_{dt}). Envelope plot (Fig.8) was divided into small increments. Using eqs. (17-19) value of envelope function E(t) was calculated. Cumulative value of E(t) was calculated at each interval and these all values are divided by final sum which give cumulative probability density function from zero to one. Considering total duration as three hundred sixty degree, phase angles for every time steps were determined randomly using probability density function. Phase angles can be obtained from previous earthquake records. However, there are no recorded earthquake acceleration histories for the region. Thus, random phase angles estimated from envelope function were used. At first, Fourier amplitude F_k is assumed unity. From, Fast Fourier Transform (FFT), accelerations at each interval was calculated. Accelerations were obtained from Inverse Fourier Transform. To make the simulated ground motion similar to natural earthquakes, the acceleration obtained from inverse Fourier transform were multiplied by envelope function. Using the calculated accelerations, response spectra was determined and compared with original spectra called target spectra. Ratio from simulated spectra to target spectra at each interval was obtained. New Fourier amplitude was then calculated multiplying old amplitude by obtained ratio. Again, FFT were calculated and accelerations were determined. The process was repeated until the simulated spectra and target spectra fit well. The schematic diagram of whole process is shown in Fig. 10.

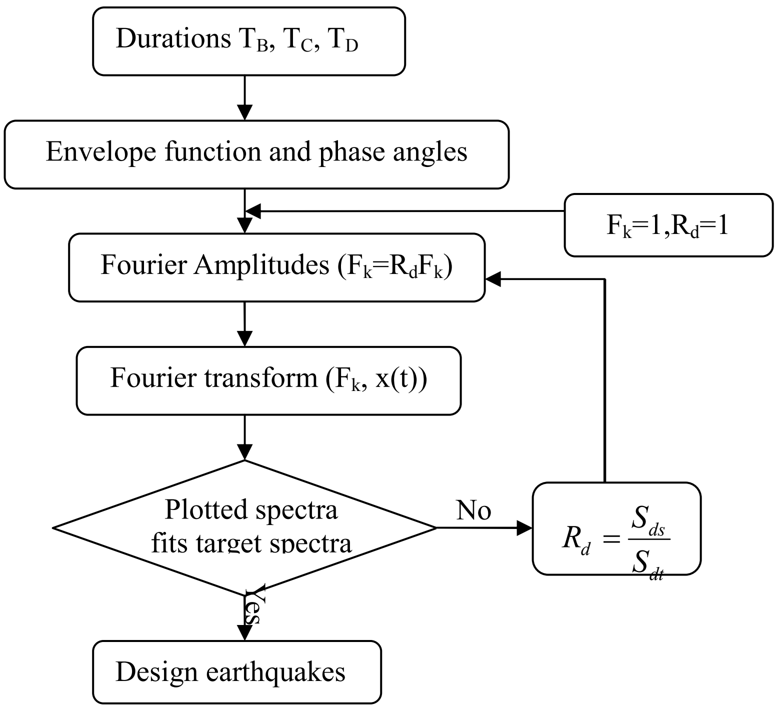

Fig. 10 Flow chart for generating acceleration histories

The accelerations histories obtained from this procedure for three probabilities of exceedences have been plotted in Fig. 11. From simulated acceleration histories acceleration response spectra were calculated and plotted against target spectra (Fig.12). For target peak ground accelerations are taken at zero period. But, for simulated spectra, plotting starts from 0.1 sec. for 975 and 475 years return periods and 0.05 sec. for 98 years return period. However, the spectra from simulated earthquake and originally calculated from attenuation law are in good agreement. In real earthquakes, accelerations start from zero, increase gradually, attains peak values and decrease to zero finally. Simulated earthquakes also look similar to natural earthquakes. Amplitudes and nature of simulated ground motions are totally depend on target spectra.

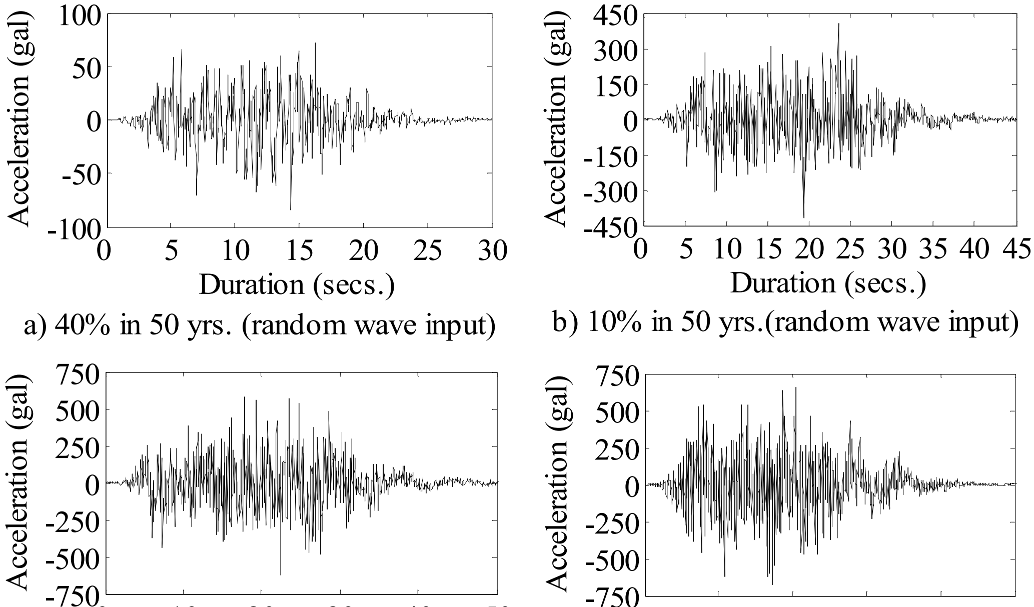

a) 40% in 50 yrs. (random wave input)

b) 10% in 50 yrs.(random wave input)

c) 5% in 50 yrs. (random wave input)

d) 5% in 50 yrs. (Kobe 1995 input)

Fig. 11 Simulated acceleration history for various return periods

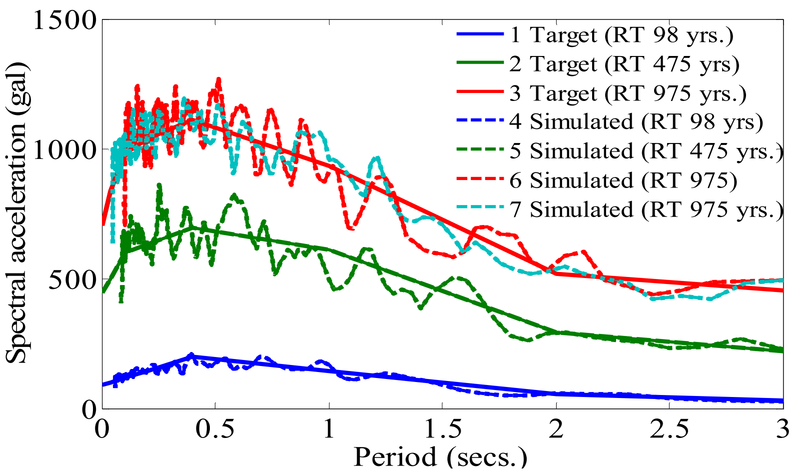

Fig. 12 Comparison of simulated and target spectra

In order to see the differences of simulated ground motion from real earthquake and randomly occurred earthquake, a simulated earthquake ground motion for 5% probability of exceedence in 50 years has been shown in Fig. 11-d. Input was given Kobe 1995 earthquake. When it is fitted with 5% probability of exceedences in 50 years, the original earthquake completely changes its shapes according target spectrum. Thus, whatever is the input either real earthquake random occurrences there are many possibilities, however, the maximum amplitude of acceleration in both case are almost similar (Fig.11 c-d).

DISCUSSION

Probabilistic seismic hazard estimate for a region where earthquakes data are missing has been done. There are many small faults around the big Himalayan thrust. But sufficient historical data are not available and available earthquake data does not satisfy the current intra-plate slip. Many of the faults are empty of historical earthquakes. However, they are the surface evidences of rupture occurred in its history. The method employed here combines three parts; historical earthquakes, faults and intra plate slip and estimate the probable hazard for the region. The density of earthquakes (Fig. 2) and contour plot (Fig.4-6) shows that the eastern and western part may experience larger accelerations than the central part. Then probabilistic spectra for the city Pokhara has been plotted (Fig. 7). Probabilistic earthquakes were obtained for weighted average duration which obtained from significant duration multiplied by weights of deaggregation and taken average for all durations corresponding to specified return period. Previous researchers have also given efforts to estimate risk consistent ground motion for example Kameda and Nojima 1988. Simulation of ground motion has been carried out focusing the characteristic or significant earthquakes. The method employed here through deaggregation is different than others. If we look at the deaggregation plot (Fig. 9), we can get magnitude and distance for significant earthquake corresponding to specified return period as a whole. The method employed here considers through the entire possible earthquakes that fall in the specified highest weight in the plot. Even though it is the highest, it may have just 10% or less weightage in overall hazard. Thus the bins other than highest weight have significant contributions. Few significant earthquakes lack to represent probabilistic earthquake for return period and simulate equivalent earthquake. Thus it differs from other estimates which are based on significant or characteristic earthquakes. This method can be useful to estimate hazard where sufficient data are not available.

CONCLUSION

Peak ground acceleration for three probabilities of exceedences were calculated and contours have been plotted. Accelerations are far higher than previously calculated by BECA 1993. Thus Revision of hazard estimate is necessary to incorporate in seismic codes. As a typical example probabilistic spectra for Pokhara city have been plotted. For the city, three separate probabilistic earthquakes were simulated. These earthquakes can be used for dynamic analyses for different life span structures. In usual practice, acceleration histories obtained from previous earthquakes are taken. However, they can not represent certain probability of exceedences. Same earthquake can not be used for varying life span structures. Thus, either new structures or existing structures, they are designed for specific life span. Thus, these probabilistic earthquakes can be useful to design for new structures or retrofitting of existing structures.

REFERENCES

Ambraseys, N.N. and Douglas, J. (2004). "Magnitude calibration of north Indian earthquakes", *Geophysics. J. Int.*, Vol. 159, 165-206.

Atkinson, G.M. and Boore, D.M. (2003). "Empirical ground-motion relations for subduction-zone earthquakes and their application to Cascadia and other regions", *Bull. Seismol. Soc. Am.*, Vol. 93 (4), 1703-1729.

Bilham, R., and Ambraseys, N. (2005). "Apparent Himalayan slip deficit from the summation of seismic moments for Himalayan earthquakes", 1500-2000, *Current science,* Vol. 88 (10), 1658-1663.

BECA World International (New Zealand) in association with SILT Consultants (P.) Ltd. (Nepal), TAEC Consult (P.) Ltd. (Nepal), Golder Associates (Canada) and Urban Regional Research (USA) (1993). "Seismic Hazard Mapping and Risk Assessment for Nepal".

Feldl, N., and Bilham, R. (2006). "Great Himalayan earthquakes and the Tibetan plateau." *Nature Publishing Group*, 444(9), 165-170.

Hank, T.C., and Kanamori, H. (1979). "A moment magnitude scale." *Journal of Geophysics Res*., **84**, 2348-2350.

Jouanne, F., Mugnier J. L., Gamond, J.F., Le Fort, P., Pandey, M.R., Bollinger, L., Flouzat, M., Avounac, J.P. (2004). "Current Shortening across the Himalayas of Nepal", *Geophysics. J. Int.*, Vol. 157, 1-14.

Kameda, H. and Nojima, N., (1988). "Simulation of risk-consistent earthquake motion", *Earthquake Engineering and Structural Dynamics*, Vol. 16, 1007-1019.

Kempton, J. J. and Stewart, P. J. (2006). "Prediction equations for significant duration of earthquake ground motions considering site and near-source effects", *Earthquake spectra*, Vol. 22(4), 985-1013.

Kramer, S.L. (1996). "Geotechnical earthquake engineering", *Prentice-Hall International series in Civil Engineering and Engineering Mechanics.*

Kumar, S., Wesnousky, S.G., Rockwell, K.T., Briggs, R.W., Thakur, V.C, and Jayangondapernumal R. (2006). "Paleoseismic evidence of great surface-rupture earthquakes along the Indian Himalaya." *Journal of Geophysical research*, 111**.**

Lave, J., Yule, D., Sapkota, S., Basnet, K., Madan, C., Attal, M., and Pandey, R. (2005). "Evidence for a great medieval earthquake (1100 A.D.) in the central Himalayas", *Science* www.sciencemag.org, Vol. 307.

Mcguire, R. K. (2004). "Seismic hazard and risk analysis." E*arthquake Engineering Research Institute, MNO-10*

Parajuli, H., Kiyono, J., Scawthorn, C. (2007). Probabilistic seismic hazard assessment of Kathmandu, *Proceedings of twentieth KKCNN symposium on civil engineering*, Jeju, Korea

Stepp, J.C. (1972). "Analysis of completeness of the earthquake sample in the Pudet Sound area and its effect on statistical estimates of earth

Wells, D.L. and Copersmith, K.J. (1994). "New empirical relationships among magnitude, rupture length, rupture width, rupture area, and surface displacement." *Bull. Seismol. Soc. Am*., **84**, (4), 974-1002.

Woo, W. (1996). "Kernel estimation methods for seismic hazard area source modeling", *Bull. Seismol. Soc. Am.*, Vol. 86 (2), 353-362.

大崎順彦　1994. 新・地震動のスペクトル解析入門　鹿島出版会

(Submitted: May 30, 2008)
(Accepted: September 18, 2008)